1 # Adaptive introgression during environmental

2 # change can weaken reproductive isolation

3

4 *Gregory L. Owens[1]*, Kieran Samuk[2]*

5

6 [1] Department of Integrative Biology, University of California, Berkeley.

7 Berkeley, California, USA, 94720.

8 [2] Department of Biology, Duke University.

9 Durham, NC, USA, 27708.

10

11 *Corresponding author, gregory.lawrence.owens@gmail.com

Abstract

Anthropogenic climate change is an urgent threat to species diversity. One aspect of this threat is the collapse of species reproductive barriers through increased hybridization. The primary mechanism for this collapse is thought to be the weakening of ecologically-mediated reproductive barriers, as demonstrated in many cases of "reverse speciation". Here, we expand on this idea and show that adaptive introgression between species adapting to a shared, moving climatic optimum can readily weaken *any* reproductive barrier, including those that are completely independent of climate. Using genetically explicit forward-time simulations, we show that genetic linkage between alleles conferring adaptation to a changing climate and alleles conferring reproductive isolation (intrinsic and/or non-climatic extrinsic) can lead to adaptive introgression facilitating the homogenization of reproductive isolation alleles. This effect causes the decay of species boundaries across a broad and biologically-realistic parameter space. We explore how the magnitude of this effect depends upon the rate of climate change, the genetic architecture of adaptation, the initial degree of reproductive isolation, the degree to which reproductive isolation is intrinsic vs. extrinsic, and the mutation rate. These results highlight a previously unexplored effect of rapid climate change on species diversity.

Introduction

Global climate change (GCC) is expected to be an increasingly important stressor in the next century (Thomas et al. 2004, Hoffmann and Sgro 2011). GCC can lead to

1

33 significant fitness costs or extinction if populations cannot adjust their ranges (e.g. via

34 migration) or adapt to the changing climate (Jump and Penuelas 2005; Zimova et al.

35 2016). Apart from its direct effects on species fitness, GCC can also profoundly alter the

36 basic ecological functioning of ecosystems e.g. via changes in phenology or species

37 composition (Walther et al. 2002). As such, GCC represents an existential threat to

38 biological diversity, at the level of populations, species, and ecosystems. Considering

39 the central role of biological diversity in the functioning of evolutionary and ecological

40 processes, understanding the full biological effect of GCC remains a key problem.

41   One potential effect GCC is increased interspecies hybridization, which can

42 itself precipitate further loss of biodiversity (Rhymer and Simberloff 1996, Todesco et al.

43 2016). Such hybridization can cause a common species to subsume a rare species

44 (Oliveira et al. 2008; Beatty et al. 2014; Vallender et al. 2007) or the collapse of multiple

45 species into a single hybrid swarm (Taylor et al. 2006). In both cases, genetic and species

46 diversity are lost. GCC may also precipitate the collapse of species boundaries by

47 breaking down spatial, temporal or behavioural premating barriers (Chunco 2014). At

48 the simplest level, range shifts can bring together species that may have no other

49 significant barriers (e.g. Garroway et al. 2010). Reproductive barriers relying on the

50 timing of life-history events are also susceptible to climate change which can increase

51 the temporal overlap between species (e.g. Gerard et al. 2006). Furthermore, behavioural

52 isolation may rely on environmental cues disrupted by GCC, as in spadefoot toads in

53 which water conditions influence mate choice (Pfennig 2007). The breakdown of these

54 barriers may lead to loss of more rare species under GCC, or the collapse of sister

55   species, as has been seen in smaller localized environmental shifts (Taylor et al. 2006;

56   Vonlanthen et al. 2012).

57   While perhaps unfamiliar to many workers in the field of climate change science,

58   there is a rich theoretical literature dedicated to the study of the dynamics of

59   interspecific hybridization and gene flow (reviewed in e.g. Abbot 2013 and Seehausen

60   2013). Often framed in the context of the evolution and maintenance of reproductive

61   isolation (i.e. speciation), this literature has provided many key insights germane to the

62   study of climate change induced hybridization. For example, hybrid zone models have

63   shown that universally adaptive alleles readily introgress across hybrid zones, while

64   alleles that cause reproductive isolation generally resist introgression (Barton 1979,

65   Gompert et al. 2012, Barton 2013). Other modelling efforts have revealed that depending

66   on the balance between reproductive isolation and shared ecological selection,

67   introgression can cause previously isolated populations to remain isolated or collapse

68   into hybrid swarms (e.g. Buerkle 2000). Further, the balance between divergent natural

69   selection, gene flow and reproductive isolation has been extensive explored in the

70   theoretical speciation literature (see Barton 2013 and references therein). However there

71   has thus far been poor integration between models of reproductive isolation and models

72   of adaptation to climate change.

73   The fact that introgression can transfer alleles between species has led to the

74   idea that hybridization could facilitate adaptation to GCC through the transfer of

75   adaptive alleles between species, i.e. adaptive introgression. This has traditionally been

76   studied in the context of species/populations with pre-existing differential adaptation to

77   the changing climate variable; for example a warm adapted species transfering alleles to

78 a cold adapted species (e.g. Gómez et al. 2015). In this example, one species acts as a

79 pool of alleles preadapted to a future climatic optimum. Importantly, in these types of

80 models, introgression is being driven by selection and not demographic processes or

81 perturbations of prezygotic isolation, as seen in other models where climate change

82 drives hybridization.

83   What has not been appreciated in previous models of adaptation to a changing

84 climate is that during a rapid environmental shift, segregating variation within two

85 reproductively isolated species could theoretically undergo adaptive introgression even

86 if neither species is particularly preadapted to the environmental shift. We propose that

87 climate-induced adaptive introgression could readily occur in most species because (1)

88 the identity of the particular alleles involved in climatic adaptation are likely

89 idiosyncratic in each species/population, and (2) these alleles could, in principle, be

90 globally adaptive under a GCC scenario. Indeed, segregating climate adaptation alleles

91 (or linked blocks of alleles) could easily be strong enough to outweigh the fitness costs

92 of any linked reproductive isolation alleles. As a side effect, reproductive isolation

93 alleles could readily be homogenized between species, reducing reproductive isolation

94 and precipitating the collapse of species boundaries. This scenario dramatically

95 increases the likelihood of GCC-induced introgression from populations differing in

96 altitude or latitude, to nearly any parapatric pair capable of hybridization, even if

97 reproductive isolation is initially high.

98   Here, we direct testly of the role of climate-induced adaptive introgression in

99 degrading reproductive barriers using state-of-the-art forward time population genetic

100 computer simulations. We envision a scenario in which two species are initially

101   reproductively isolated (but capable of limited hybridization) and must cope with an

102   extreme shift in the environment. We explore the parameter space under which

103   adaptation to a shifting climatic optimum drives a reduction in reproductive isolation.

104   We interpret these results in the context of the future anthropogenic climate change

105   and the loss of species diversity.

106   ## Methods

107   *Conceptual model*

108   We consider the scenario of two parapatric species inhabiting demes in two

109   different habitats. These species exchange migrants at a low level, but reproductive

110   isolation via local adaptation (i.e. extrinsic postzygotic isolation and immigrant

111   inviability) is strong enough to prevent substantial introgression. We imagine that these

112   two species must also cope with constant adaptation to a shared oscillating "climate"

113   optimum. This climatic optimum does not not directly affect the degree of local

114   adaptation and/or reproductive isolation, i.e. reproductive isolation is completely

115   independent of the direct effects of climate. The climate oscillation continues for a long

116   initial burn in period, during which alleles conferring adaptation to climate accumulate

117   in each species. After this period, the oscillation ends and the climatic optimum begins

118   rapidly increasing at a constant rate, as is expected under projections of anthropogenic

119   climate change.

120   We hypothesize that if the rate of change in the climatic optimum is sufficiently

121   high, selection for migrant alleles conferring increased climate tolerance will

122   overwhelm the negative fitness effects of linked reproductive isolation alleles. This will

123 cause the erosion of reproductive isolation between species and increase the chance of

124 speciation reversal. Importantly, we expect this outcome even when the strength of

125 ecological selection mediating reproductive isolation itself is orthogonal to the strength

126 of climate-mediated selection.

127

128 *Model details*

129   We implemented the above conceptual model as a genetically explicit Wright-

130 Fisher model in SLiM 3.0 (Haller and Messer 2018). As in all Wright-Fisher models,

131 population sizes are constant, all fitness is relative and extinction is impossible. The

132 details of our implementation are depicted graphically in Figure 1 and a list of

133 simulation parameters and their values are detailed in Table 1. We simulated two

134 diploid populations of constant size Ne, with a constant migration rate of m proportion

135 migrants per generation. Each individual was initialized with 99999 genetic loci

136 contained on a single chromosome with a uniform recombination rate of r between loci.

137 We initially scaled the recombination rate so that the entire genome was 100 cM in

138 length, but also explored varying recombination rates up a genome size of 1000 cM (see

139 Results). We modelled local adaptation in the two populations as l_{EX} divergently

140 selected alleles at loci evenly spaced across the chromosome, with each population fixed

141 for a different allele. Divergently selected alleles imposed a fitness cost of s_{RI} when not

142 found in their home population/habitat, modelling extrinsic postzygotic isolation.

143   In addition to extrinsic postzygostic isolation, we also modelled intrinsic

144 postzygotic isolation using two-locus Bateson-Dobzhansky-Muller incompatibilities

145 (Bateson 1909, Dobzhansky 1936, Muller 1942). These epistatic incompatibilities were

146   modelled as a fitness cost of s_{RI} scaled by the number of negatively-interacting pairs of

147   alleles from each population (see Supplementary Appendix 1 for details). When testing

148   the effects of BDMs, we maintained a constant number of total reproductive isolation

149   loci, but varied the proportion of loci that were extrinsic or BDM loci (*l*). We also

150   explored the effect of the total number of RI loci (i.e. the genetic architecture of RI *per*

151   *se*) on the potential for adaptive introgression/hybridization. To keep the total

152   magnitude of RI similar between simulations, we always co-varied s_{RI} so that the s_{RI} x *l*

153   was held constant. To allow for fine-scale view of introgression, we tracked ancestry

154   was using 100 neutral alleles initially fixed between the populations, spread evenly

155   across the genome. All alleles of selective/phenotypic effect were codominant with

156   dominance = 0.5.

157   In addition to reproductive isolation, individual fitness also depended on their

158   phenotypic distance from a climatic optimum. This optimum was initially 0, and during

159   the burn in period oscillated from -5 to 5 (in arbitrary units) every 500 generations based

160   on the formula: $sin(\pi * generation / 500) / 5$. The individual phenotype was determined by

161   alleles at QTL-like climate loci which could appear via mutation at all sites other than

162   RI or ancestry tracking loci (i.e. 99899 - *l* sites). Climate QTL mutations occurred at a

163   rate μ per locus per sample per generation and their phenotypic effect was drawn from a

164   gaussian distribution with a mean of zero and a standard deviation of QTL_{SD}.

165   Conceptually, these QTL climate alleles modify whether an individual is "hot" (positive

166   effects) or "cold" (negative effects) adapted.

167   The first step of the simulations was a burn-in of $10Ne$ generations to simulate

168   the generation of standing genetic variation under normal climatic conditions. At the
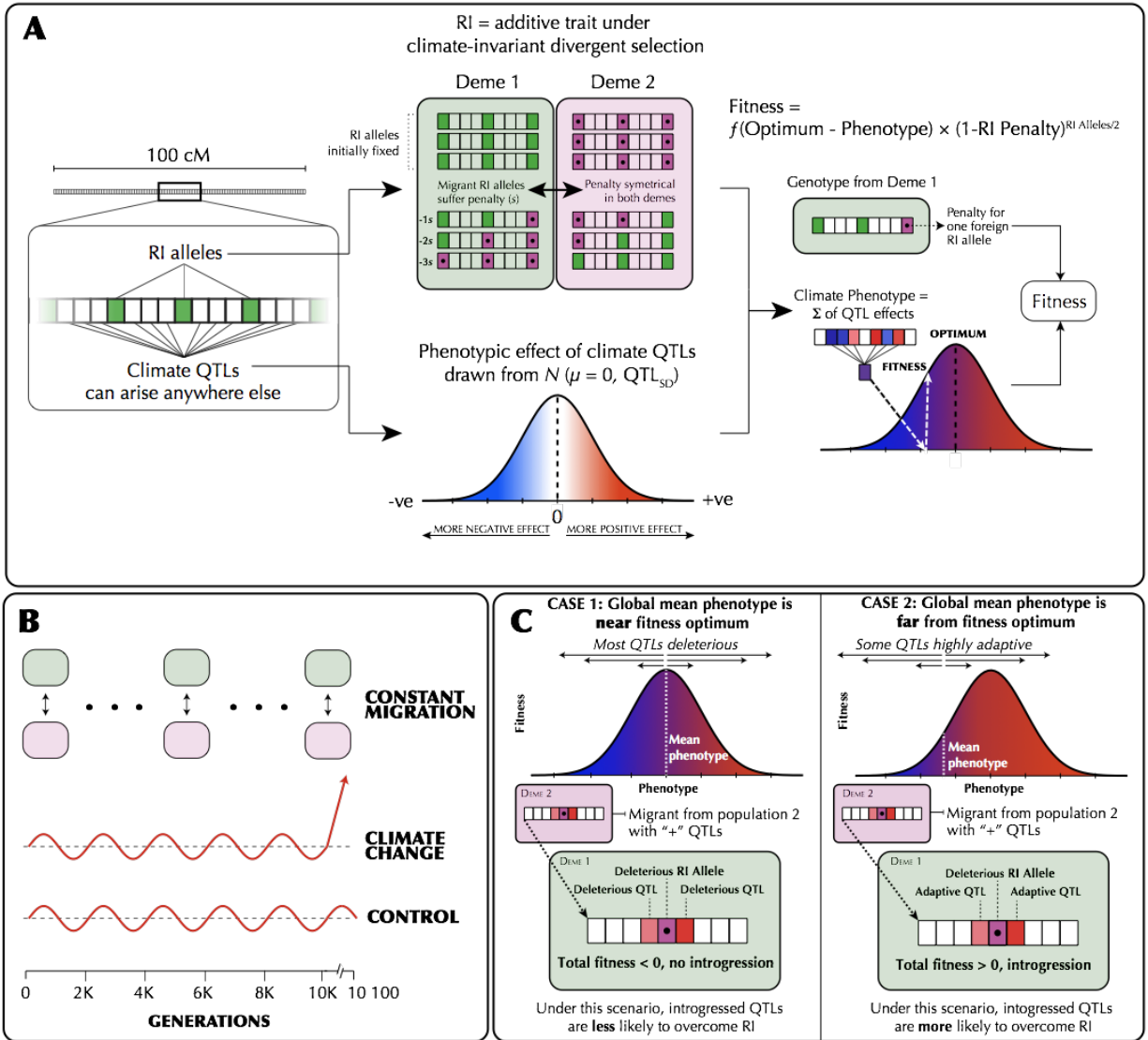
7

169 end of the burn-in period, the complete state of each replicate simulation was saved.

170 Each simulation was then continued under both a "control" and climate change

171 scenario for an additional 100 generations. In the control scenario, the environmental

172 oscillation continued as normal. In contrast, under the climate change scenario the

173 phenotypic optimum increased by a rate of Δ each generation without oscillation. In

174 each generation we recorded the average degree of reproductive isolation, mean fitness,

175 the mean and standard deviation of the climate phenotype and the amount of

176 introgressed ancestry for each population. Reproductive isolation (RI) was calculated

177 accounting for the extrinsic and BDM loci. For extrinsic loci, RI was the difference in

178 fitness for an average individual in their home habitat vs. the foreign habitat. For

179 BDMs, since fitness penalties occur only in F1 hybrids and beyond, we calculated the

180 expected average magnitude of BDM fitness costs based on Hardy-Weinberg

181 expectations in F1s (Supplementary Appendix 1). Finally, for each simulation we report

182 the mean introgressed ancestry and reproductive isolation between the start and end of

183 control and test scenarios, as well as the mean rate of phenotypic change in Haldanes

184 for the test scenario. A Haldane is a measure of evolutionary change in log mean trait

185 value in units of standard deviation of that log trait (Gingerich 1993). All formulas used

186 in the simulation are presented in the Supplementary Appendix and all code for

187 underlying simulations is available at

188 https://github.com/owensgl/adaptive_introgression.

189   To explore the parameter space under which adaptive introgression mediates RI

190 collapse, we systematically varied the following parameters: mutation rate (μ), migration

191 rate (m), strength of divergent selection (s_{RI}), the number of divergently selected loci (n_{RI}),

192   the proportion of BDMs (pr_{BDM}), the standard deviation of QTL effect sizes (QTL_{SD}) the

193   recombination rate (r), and the rate of climate change (Δ). We varied each parameter

194   independently and kept the other parameters at a default value known to permit a low

195   level of introgression in preliminary tests (Table 1). Each parameter set was replicated

196   100 times. All analyses were carried out in R 3.5.1 (R Core Team 2018) and plotting was

197   done using ggplot2 (Wickham 2016).

198   Finally, while our primary goal was testing the detrimental effects of

199   hybridization, we also examined the potential *beneficial* effects of climate change

200   induced introgression, i.e. to what degree introgression facilitates adaptation. To do

201   this, we ran simulations varying the rate of climate change with (m=0.01) or without

202   (m=0) migration. At the last generation (gen=10,100), we compared the average climate

203   phenotype to the current phenotypic optimum. We defined "adaptational lag" as the

204   difference between these values divided by the rate of climate shift. This represents how

205   many generations behind the current generation that the population is adapted to. For

206   example, assume the optimum increases by 2 per generation and is currently 100, if the

207   average phenotype is 90, then the adaptational lag is 5 (e.g. (100 - 90) / 2).

208

209

Figure 1 | (A) The genetic architecture of adaptation and speciation in the model. From left to right: Each individual has a single 100-1000 cM chromosome, over which reproductive isolation (RI) loci occur at regularly-spaced intervals. These loci are initialized with RI alleles (at 100% frequency) that confer local adaptation to one of two initial demes (depicted as green or purple/dotted alleles, corresponding to Deme 1 or Deme 2 environments). Both demes are of equal size (Ne = 1000). All non-RI loci (depicted as white/transparent loci, initially) have the potential to give rise to climate-adaptation alleles. The phenotypic effects of each these alleles are drawn from a normal distribution (shown as a gradient from blue to white to red). An individual's climate phenotype is the sum of the phenotypic effects of its climate QTLs (pure additivity). The fitness of each individual is a function of the number of foreign RI alleles and the phenotypic distance of that individual from the environmental optimum, with the climate fitness landscape modelled as a gaussian distribution (shown as a gradient from blue to red). (B) The course of the simulation. Migration rate and population size of the two demes is held constant. In each replicate

223   simulation, the fitness optimum fluctuates regularly for a 10 000-generation burn-in period. The state of

224   the initial population is then duplicated and subjected to 100 additional generations of (1) a climate

225   change scenario in which the climatic optimum rapidly shifts in a single direction and (2) a control

226   scenario in which the optimum continues its fluctuation course. (C) The conditions under which adaptive

227   introgression overwhelms RI. On the left, if the two populations are able to individually track the climatic

228   optimum, newly-arising climate alleles are only able to exert either weakly positive or (more commonly)

229   negative effects on fitness due to overshooting the optimum. In contrast, on the right, if the populations

230   cannot effectively track the optimum, there is scope for climatic alleles to have large positive fitness

231   effects. If these fitness effects are sufficiently large, these alleles can overwhelm the negative fitness

232   effects of linked RI alleles and introgress between demes, degrading overall reproductive isolation.

233

234   **Table 1** | Parameters of the adaptive introgression simulations. For each set of simulations, each

235   parameter was set to the starting value which was varied from the minimum to maximum value by the
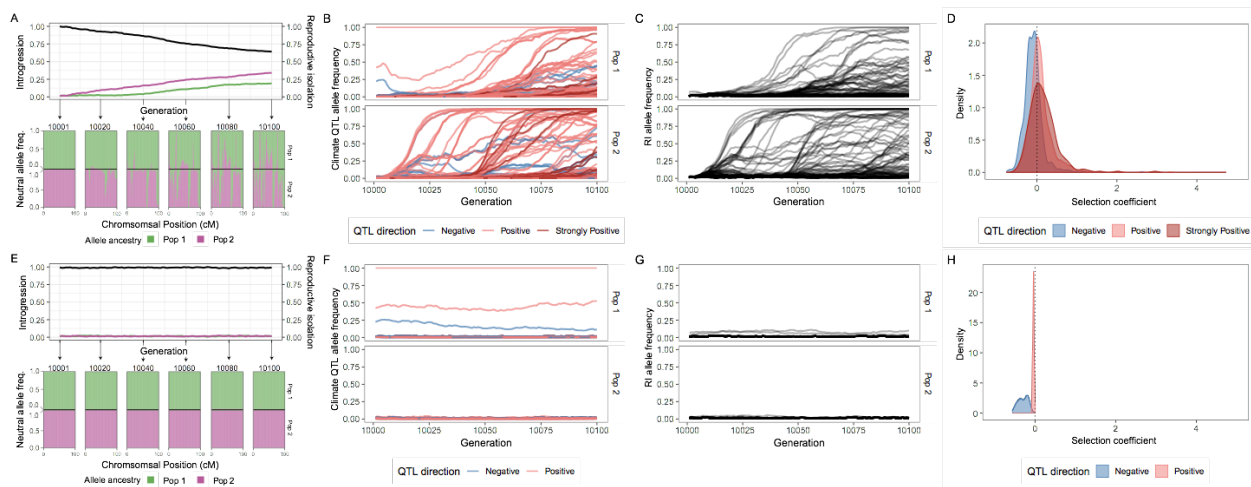
236   specified increment.

Parameter	Symbol	Starting value	Range, Increment
Migration rate (proportion migrants/generation)	m	0.01	0.0-0.1, 0.001
Strength of RI	s_{RI}	0.01	0.004-0.0195, 0.0005
Number of RI loci	l	100	5-100, 5
Mutation rate (mutations/sample/locus/generation)	μ	1e-7	$1e^{-8}$-$5e^{-7}$, $1e^{-8}$
Climate QTL standard deviation	QTL_{SD}	1	0.1-5.0, 0.1
Delta	Δ	1	0.1-3, 0.1
Recombination rate	r	1e-5	$1e^{-5}$-$5e^{-5}$, $1e^{-6}$
Proportion BDM loci	BDM_{pr}	0	0-0.96, 0.04
Population size	N_e	1000	-
Environmental fitness standard deviation	$sd_{climate}$	2	-
Burn in generations	-	10000	-
Shift generations	-	100	-
Replicates	-	100	-
Loci on chromosome	-	99999	-

| Burn in oscillation rate | f | 1000 | - |
| Burn in oscillation height | a | 5 | - |

Results

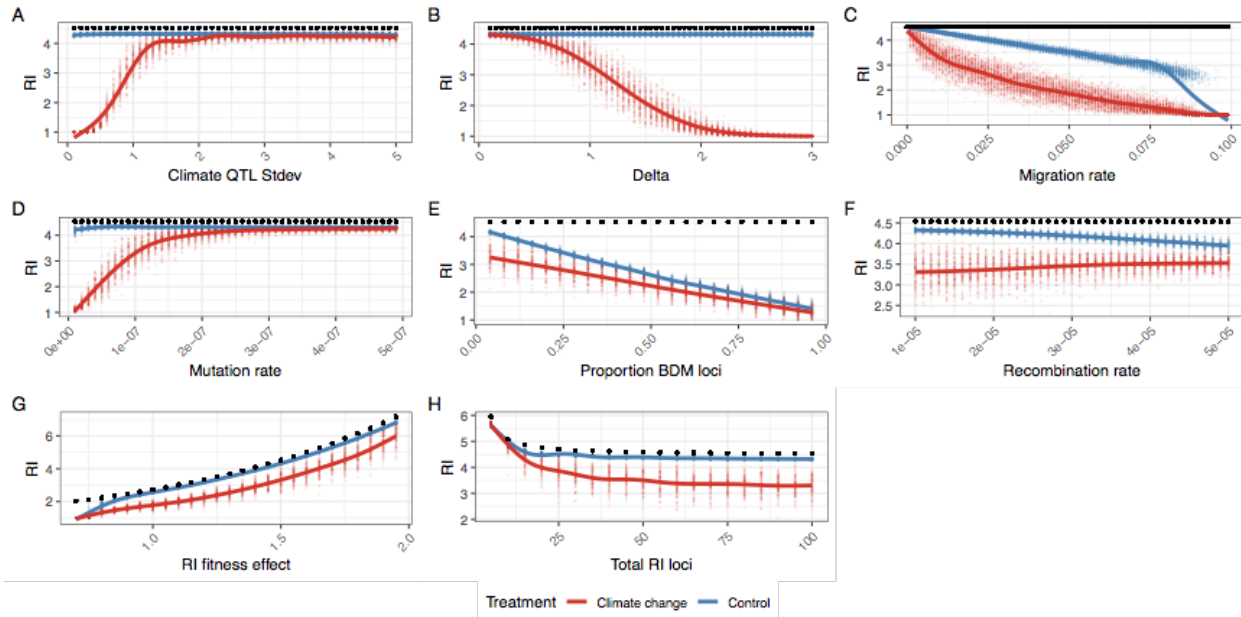*Rapid climate change and adaptive introgression facilitates collapse of species boundaries*

When climate change is rapid, we find that adaptive introgression of climate QTL alleles rapidly drives the homogenization of allele frequencies at linked RI loci between species. Figure 2 visualizes one example simulation where after 100 generations of climate change, RI is degraded to nearly half its original strength (Figure 2A) and introgressed climate QTL alleles are common (Figure 2B). As climate QTL alleles move between populations, RI and neutral alleles hitchhike along with them resulting in substantial genome-wide introgression (Figure 2A & 2C). In contrast, in the control scenario without climate change, RI remains intact and introgression is minimal (Figure 2 E-H).

Figure 2 | A single example simulation with Δ = 1.5, illustrating the climate driven adaptive introgression. Panels A-D present the test climate change scenario, while E-H are the control scenario. (A & E) The upper half is the average introgressed ancestry for each population (purple and green) and the average reproductive isolation between populations (black). The lower half is the ancestry for neutral loci during

253 the post-burn in period at 20 generation intervals. The top and bottom parts of this portion represent
254 population 1 and 2 respectively. (B & F) The allele frequency trajectory for introgressed climate QTL color
255 coded by QTL strength. Color codes QTL effect; -ve phenotypic effect (blue), +ve effects (light red) or
256 large +ve effect (>2, dark red). (C & G) The allele frequency trajectory for introgressed RI alleles (D & H)
257 The distribution of selection coefficients on QTL loci per population per generation. Color groups
258 represent QTL with -ve phenotypic effect (blue), +ve effects (light red) or large +ve effect (>2, dark red).
259 Plot is filtered to only include loci with allele frequency < 0.9 and > 0.1.
260
261   For a wide range of parameters we find decreased reproductive isolation and

262 increased introgressed ancestry under the climate change scenario (Figures 3 and S1).

263 This effect is enhanced by reduced levels of genetic variation; both reducing mutation

264 rate and reducing the standard deviation of the climate QTL effect size increases the

265 likelihood and magnitude of adaptive introgression (Figure 3A, Figure 3D). Increased

266 migration generally causes increased RI loss, although high migration degrades RI even

267 in the absence of climate shifts (Figure 3C). Interestingly, increasing the average fitness

268 effect of RI loci has minimal effect on the amount of RI lost, although below a

269 threshold, populations merge and all RI is lost during the burn in period (Figure 3G).

270 Recombination rate has two effects; during the burn in, increased recombination allows

271 for more RI loss, while during climate change decreased recombination leads to slightly

272 more RI loss (Figure 3F). When varying the genetic architecture of RI, we find that fewer

273 strong RI loci, lead to less RI loss (Figure 3H). We find that intrinsic isolation is much

274 less effective at maintaining RI during the burn in period, consistent with previous

275 simulations (Bank et al. 2012). Climate change increases the amount of introgression

276 and RI loss when intrinsic isolation is present unless populations are already completely

277 merged (Figures 3E, S1E). Lastly, increasing the rate of climate change in the test

278 scenario increases the amount of adaptive introgression (Figure 3B).

279

280

281 **Figure 3** | The average reproductive isolation at generation 10,100 for climate change (red) and control
282 simulations (blue), while varying individual parameters. RI is defined as the home fitness advantage which
283 is the fold fitness advantage for the average sample in its home environment compared to the alternate
284 environment based on divergent selection and BDM loci. A value of 1 means equal fitness in both
285 environments and there is no RI. The black dot is the initial and maximum level of RI for each simulation.
286 Individual parameters were varied to show the effect of (A) climate QTL effect size standard deviation, (B)
287 optimum shift per generation (delta), (C) migration rate, (D) climate QTL mutation rate, (E) proportion of
288 RI loci that are BDM instead of extrinsic, (F) the recombination rate, (G) the fitness effect of each RI loci
289 and (H) the number of RI loci.

290

291 *Simulation parameters fall within realistic ranges*

292   To better connect our simulation results with observations from natural

293 populations, we measured the rate of phenotypic evolution in the test scenario in

294 Haldanes (standard deviations per generation). We find that most simulations had

295 average evolutionary rates ranging from 0.01 to 0.06 Haldanes and are well within the

296 range of empirical estimates from natural populations (Hendry et al. 2008). That said, in

297 simulations with very high rates of climate change ($\Delta > 2.5$), we found large and erratic

298 evolutionary rates. For many of these simulations, one or both species failed to track the

14

299　changing environment causing fitness of all individuals to fall to zero and end the

300　simulation.

301　　　　In example simulations, we found that 99.3% of the realized selection coefficients

302　for introgressed climate QTL alleles fell below 1 (Figure 2D). QTL alleles with positive

303　and strongly positive phenotypic effects were more likely to have positive selection

304　coefficients, consistent with the importance of the climate optimum.

305　*Beneficial effects of introgression*

306　　　　 We find that migration can reduce adaptational lag when climate change is

307　moderate or high (Figure 4). This effect is particularly strong when climate change is

308　rapid.

309
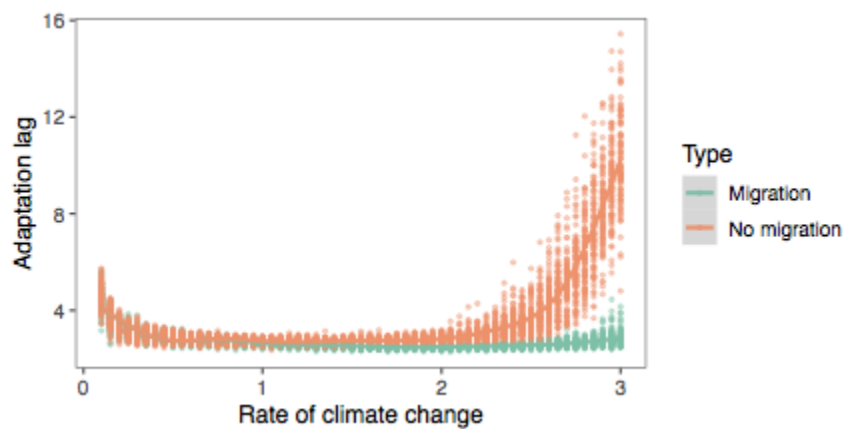
310
311　**Figure 4** | The adaptational lag at the final generation for simulations with (m=0.01) and without
312　migration (m=0). Adaptational lag is defined as the phenotypic optimum minus the phenotypic mean
313　divided by the rate of change in optimum, and represents how many generations behind the changing
314　optimum that the population is.

315　# Discussion

316　　　　Global climate change is expected to have wide-ranging detrimental effects on

317　biodiversity. The movement of beneficial alleles between species, i.e. interspecific

adaptive introgression, is likely to increasingly relevant as the climate warms. In spite of increased interest in adaptive introgression per se, we still have a poor understanding of the incidental effects of adaptive introgression on the integrity of species boundaries. Our simulations have shown that it is possible for adaptation to a common, changing environment to cause introgression and speciation reversal. Importantly, we observed this effect in scenarios where the mechanism of RI is itself completely independent of the changing climate.

Will adaptive introgression lead to speciation reversal?

In our simulations, several parameters had a strong effect on the amount of introgression. When adaptive variation is limited, RI is initially weak, or environmental change is rapid, complete genetic homogenization is likely. In these cases, RI is completely degraded and would clearly represent speciation reversal in a natural system. In more moderate parts of parameter space, introgression is increased during environmental change, but populations do not completely homogenize (Figure S1). In these cases, RI is still eroded between populations (Figure 3). Importantly, we believe our estimates of RI loss are likely somewhat conservative, because we do not include any additional factors that would contribute to species collapse (e.g. cases where RI is directly affected by a change in climate).

We found that in the absence of divergent selection intrinsic epistatic isolation (BDM incompatibilities) were unable to maintain RI during the burn in period. This result is consistent with previous modelling of parapatric speciation (Barton & Bengtsson 1986, Bank et al. 2012, Lindtke & Buerkle 2015). Consistent with their effect

in the burn in period, during climate change, introgression and RI loss is enhanced

when intrinsic RI is present. Thus, although we have focused on extrinsic RI, intrinsic

RI is also susceptible to adaptive introgression.

The ultimate question of which species are in danger of reverse speciation is

dependent on a multitude of interacting factors and is beyond the scope of this paper,

but we can highlight several risk factors.

(1) For hybridization to be an issue, a potential hybridizing species must be at least

in parapatry. Surveys have estimated the percent of species that hybridize with at

least one other congener to be around 10-25%, although if climate change

disrupts species ranges or premating isolation, that number may increase (Mallet

2005).

(2) The rate of environment change and the steepness of the changing fitness

landscape. Species with broader climate niches will be less susceptible because

they will be under weaker selection.

(3) The genetic architecture of climate adaptation in the species. Species with

numerous large effect climate adaptation alleles segregating within their gene

pool will be more able to adapt to the changing climate *without* introgressed

alleles. Low diversity species will be more susceptible and reliant on adaptive

introgression.

(4) The genetic architecture of reproductive isolation between species. Species with

few large effect RI loci will be more resistant to RI decay than species with a

more diffuse and polygenic RI architecture.

363   (5) The demographic and life history of the species. Unbalanced population sizes

364   may result in one population harboring more adaptive alleles and lead to

365   unbalanced introgression. Small populations will also be more susceptible to

366   extinction due to the fitness costs of introgressed RI alleles. Features that reduce

367   effective population size, e.g. high variance in reproductive success, are also

368   likely to have reduced diversity of climate adapting alleles.

369

370   *Implications for the fate of species in changing environments*

371   Our simulations suggest that rapidly changing environments can cause the

372   collapse of species barriers in the *absence* of any direct effect on the underlying strength

373   of reproductive isolation. By design, we modelled a scenario in which the strength of RI

374   (modelled as divergent selection) is (a) invariant throughout (i.e. not reduced by

375   environmental change itself) and (b) totally orthogonal to the strength of climate-

376   mediated selection (i.e. extrinsic RI alleles do not affect the climate phenotype). This is

377   an important departure from previous work, in which the collapse of reproductive

378   isolation or "reverse speciation" occurs because RI is itself dependent on the

379   environment (e.g. trophic or sensory niche).

380   This difference has several important implications. For one, the mechanism we

381   outline here can occur in any population where adaptive introgression is possible (i.e. RI

382   is not absolute and the climate-mediated selective optimum is to some degree shared).

383   This greatly expands both the number of populations that may be susceptible to

384   introgressive collapse and the potential severity of such collapses. For example, adaptive

385   introgression could act in concert with the collapse of climate-mediated reproductive

386 barriers, accelerating collapse. Further, while we focused on extrinsic isolation, our

387 simulations show that scenarios where reproductive barriers are independent of

388 ecological context (e.g. in the case of purely intrinsic isolation) are not immune.

389   Although we have framed our discussion in the context of climate change, our

390 results are applicable to any strong, consistent, and shared selective event. These events

391 include any environmental or ecological disturbance that alters the shared selective

392 landscape of the two populations such that both populations are sufficiently displaced

393 from their selective optima (thereby increasing the average size of selection differentials

394 between genotypes, i.e. the strength of selection). One such event that has been studied

395 in natural systems is eutrophication, which has been suggested to have caused

396 speciation reversal in European lake whitefish (Vonlanthen et al. 2012). Thus far, this

397 reversal has been attributed to changes in RI as a direct result of ecological and/or

398 behavioural changes. However, if eutrophication exerts a common selective pressure on

399 a group of parapatric species (e.g. mediated through changes in water chemistry)

400 introgression could become adaptive and contribute to the collapse of species

401 boundaries. Similarly, ocean acidification could be a strong source of shared selection

402 and may induce introgression between previously well isolated species (Pespeni et al.

403 2013).

404   In contrast to our hypothesis of introgression driving species collapse, adaptive

405 introgression of an insecticide-resistance mutation in *Anopheles* mosquitoes lead to the

406 homogenization of previously differentiated genomic region, but not genome wide

407 despeciation (Clarkson et al. 2014). In this example, selection seemingly only acts on a

408 single large effect locus, rather than the polygenic architecture of climate adaptation we

409   hypothesize. This limits the amount of introgression in comparison to our simulations

410   and highlights the importance of the genetic architecture of climate adaptation.

411   *Introgression and extinction*

412   Here we've focused on the possibility of species collapse, but another more

413   common predicted effect of climate change is extinction. In our model, population sizes

414   are constant and fitness is relative, so extinction is impossible. Despite this, our results

415   do have implications for the likelihood of extinction.

416   If RI alleles contribute to local adaptation (i.e. are extrinsic), then the collapse of

417   RI must result in the spread of fitness reducing maladaptive non-local loci introgress,

418   similar to the concept of linkage drag in plant breeding (Zamir 2001). The net effect of

419   the introgression is positive in our climate change scenario, since the maladaptive

420   introgressed alleles are linked to positive climate QTL alleles, but the overall fitness of

421   the population is lower than it would be if it adapted *without* introgression. In this way,

422   adaptive introgression makes populations better adapted to the changing climate, but

423   less adapted to their home niche. In the real world, this may be reflected in reduced

424   population size or growth rate and could increase the chance of extinction. This effect is

425   dependent on the amount and type of RI loci swept to fixation by linkage with beneficial

426   climate QTL, which in itself will depend on the speed of fixation and amount of

427   recombination. Thus stronger selection, smaller population size or reduced

428   recombination rate will all increase linkage drag. Note that if RI is intrinsic, this doesn't

429   necessarily apply because intrinsic RI loci are only detrimental based on interactions

430   with other loci and won't have any fitness penalty if all RI alleles are homogenized by

431   introgression.

432   On the other hand, it is likely that the adaptive introgression of climate QTL

433   increases the chances that a species can adapt to a changing environment instead of

434   going extinct. Again, we can't directly address this question in our model but we do see

435   that when all introgression is prevented adaptational lag increases (Figure 4). This is

436   consistent with the larger total gene pool of adaptive variants available when gene flow

437   is possible. The magnitude of this effect will depend on the amount and architecture of

438   divergently selected loci (i.e. the potential linkage drag) as well as the diversity of

439   climate QTL alleles in each species (i.e. the effective population size).

440   *Linkage and the genetic architecture of climate adaptation*

441   A key aspect of our model is that while RI loci occur at predefined intervals in

442   the genome, climate-sensitive alleles can arise at any other locus in the genome. This

443   allows for climate-sensitive alleles to become readily linked to RI-causing alleles and

444   eventually introgress if the combined effect of positively selected climate alleles exceeds

445   the deleterious effect of the linked RI allele. The incidental establishment of this

446   linkage within the two adapting populations is a fundamental cause of later

447   introgressive collapse. This is supported by our simulations that varied the number of

448   RI loci and also incidentally varied the average degree of linkage between all climate-

449   sensitive loci and all RI loci. We found that in simulations with more RI loci, and

450   therefore a higher probability of linkage between RI and climate-sensitive loci, there

451   was greater loss of reproductive isolation. Thus, a key question is whether such linkage

452   could plausibly be established in a natural population.

453   Several lines of evidence suggest that this is likely to be true. First, the genetic

454   architecture of adaptation to a changing climate is likely to closely resemble the

455   architecture of local adaptation in general, i.e. a large number of small effect alleles with

456   a smaller number of large effect loci (reviewed in Savolainen et al. 2013). This idea is

457   directly supported by recent work showing that climatic adaptation in conifers is

458   underlain by large number of loci scattered throughout the genome, with the majority of

459   these showing modest phenotype-environment correlations (Yeaman et al. 2016).

460   Secondly, recent analyses of large human datasets support the idea that most complex

461   traits (of any kind) are probably determined by a large number of small-effect loci found

462   nearly everywhere in genome along with a handful of "core genes" (Boyle et al. 2018).

463   Thus, given that the genetic architecture of RI is itself likely to be highly polygenic

464   (further discussed in Ravinet et al. 2017), it seems highly plausible that linkage between

465   climate-sensitive alleles and RI alleles can readily occur in natural populations.

466   *The role of recombination rate*

467   Recombination rate is thought to play a key role in mediating patterns of

468   divergence and introgression in natural populations (e.g. Samuk et al. 2017, Schumer et

469   al. 2018). Specifically, regions of high recombination are thought to be less resistant to

470   gene flow because of decreased linkage between alleles conferring RI. We see this in our

471   simulations, as simulations with higher recombination rates have greater amounts of

472   introgression in both control and climate change scenarios. Interestingly, we observe a

473   slight negative correlation between recombination rate and loss of RI under the climate

474   change scenario (Figure 3, Figure S1). This effect is a direct consequence of lower

475   recombination rates leading to increased linkage between RI alleles and globally-

476   adaptive climate alleles. This increased linkage leads in turn to larger numbers of RI

477   alleles being dragged along with globally-adaptive alleles and homogenized between

478   populations. While mutations were not particularly limiting in our simulations, adaptive

479   introgression in regions of low recombination should generally require larger effect

480   alleles than introgression in regions of high recombination, particularly at the onset of

481   climate change when selection is weaker overall.

482   *The strength of climate-mediated selection*

483   A strong shared selection pressure is ultimately the key mediator of the collapse

484   of RI we observed. Was the magnitude of simulated selection necessary to cause this

485   collapse realistic? One way to assess this is to measure the magnitude of the phenotypic

486   response to selection in our simulations and compare it to estimates from natural

487   systems. In our case, the phenotypic response to selection ranged from 0.01-0.06

488   Haldanes (standard deviations per generation). This is in line with the magnitude of

489   phenotypic response observed in both natural and anthropogenically-induced selection

490   (e.g. Hendry et al. 2008). Further, this is below the theoretical threshold of 0.1 Haldanes

491   thought to result in an unsustainable long-term response to selection (for N_e = 500;

492   Lynch & Lande, 1993; Bürger & Lynch, 1995).

493   Another way of assessing the realism of our scenarios is comparing the selection

494   coefficients of climate QTL in our simulations with values measured in empirical

495   studies. We measured selection coefficients in our example simulation by comparing

496   relative fitness values for samples with and without each mutation (Appendix 1), and

497   therefore are capturing not just the effect of the climate QTL mutation, but also all

498   linked loci. Only 0.7% of introgressed climate QTL loci had selection coefficients > 1,

499   within the range of empirical values, therefore adaptive introgression is occurring

500   without abnormally high selection coefficients (Kingsolver et al. 2001).

501   Thus, the strength of selection we modelled was not particularly extreme nor

502   would it necessarily lead to the extinction of the modelled populations. It is also worth

503   noting that the estimated rate of phenotypic change in wild populations due to future

504   GCC is thought to be at least as large as the rates we described here, and are projected

505   to likely exceed 0.1 Haldanes in many cases (Gienapp, Leimu, & Merilä, 2007; Merilä &

506   Hoffman 2016). In sum, the global strength of phenotypic selection simulated here was

507   not unrealistically high, and if anything represents a conservative adaptive scenario.

508

509   *Conclusion*

510   Hybridization is a double-edged sword under rapid environmental change. It can

511   allow species access to a larger pool of adaptive alleles but linkage with RI alleles will

512   weaken overall RI and may lead to speciation reversal. Importantly, our work highlights

513   the dangers of hybridization for a much wider pool of species, not just those on range

514   margins or with existing porous species boundaries. In the longer term, we predict that

515   specific cases of speciation reversal should be linked to climate change but we also

516   predict effects before full speciation reversal. If our model is correct, we predict that

517   alleles conferring adaptation to present and future climate (e.g. heat or drought) will be

518   more likely to introgress between species. Although identifying all the loci underlying

519   climate adaptation is challenging, recent work by Exposito-Alonso et al. (2019)

520   highlights that it can be done. Such an approach can be combined with sequencing data

521   in related species to identify where introgression is occuring. Our results also suggest

522   that hybrid zones should become increasingly porous as climate adaptation alleles move

523   between species and that this effect would be stronger in regions with more dramatic

524   climate change (e.g. the arctic). This could be done by resampling previously studied

525   hybrid zones or by comparing contemporary samples to museum and herbarium

526   samples. Confirmation of these predictions would show that climate adaptation is

527   occurring through a larger multi-species gene pool and be a warning sign for the future

528   homogenization of these species.

529

537

References

539

540   Abbott, R., Albach, D., Ansell, S., Arntzen, J. W., Baird, S. J., Bierne, N., ... & Butlin, R. K.

541   2013. Hybridization and speciation. Journal of evolutionary biology, 26(2), 229-

542   246.

543

544   Bank C., Bürger R. & Hermisson J. 2012. The limits to parapatric speciation:

545   Dobzhansky–Muller incompatibilities in a continent–island model. Genetics.

546   191(3):845-863.

547   Barton N. H., 1979. The dynamics of hybrid zones. Heredity. 43(3):341–359.

548

549 Barton N. H., 2013. Does hybridization influence speciation? Journal of Evolutionary
550   Biology. 26(2):267–269.

551

552 Barton, N. & Bengtsson, B.O. 1986. The barrier to genetic exchange between hybridising
553   populations. Heredity. 57(3):357-376.

554

555 Bateson W. 1909. Heredity and variation in modern lights. Darwin and Modern Science.
556   85–101

557

558 Beatty, G.E., Barker L., Chen P.P., Kelleher C.T. & Provan J. 2014. Cryptic introgression
559   into the kidney saxifrage (*Saxifraga hirsuta*) from its more abundant sympatric
560   congener *Saxifraga spathularis*, and the potential risk of genetic assimilation.
561   Annals of Botany. 115(2):179-186.

562

563 Boyle, E. A., Li, Y. I., & Pritchard, J. K. 2017. An expanded view of complex traits: from
564   polygenic to omnigenic. Cell. 169(7):1177-1186.

565

566 Bürger R. & Lynch M. 1995. Evolution and extinction in a changing environment: a
567   quantitative-genetic analysis. Evolution. 49(1):151-163.

568

569 Buerkle, C.A., Morris, R.J., Asmussen, M.A. & Rieseberg, L.H. 2000. The likelihood of
570   homoploid hybrid speciation. Heredity 84: 441–451.

571

572 Chunco AJ. 2014 Hybridization in a warmer world. Ecology and Evolution. 4(10):2019-
573   2031.

574

575 Clarkson C.S, Weetman D., Essandoh J., Yawson A.E., Maslen G., Manske M., Field
576   S.G., Webster M., Antão T., MacInnis B. & Kwiatkowski D. 2014. Adaptive
577   introgression between Anopheles sibling species eliminates a major genomic
578   island but not reproductive isolation. Nature Communications. 5:4248.

579

580 Dobzhansky T. 1934. Studies on Hybrid Sterility. I. Spermatogenesis in pure and hybrid
581   *Drosophila pseudoobscura*. Zeitschrift für Zellforschung und mikroskopische
582   Anatomie. 21:169–221

583

584   Dobzhansky, T. H. 1936. Studies on hybrid sterility. II. Localization of sterility factors in
585   Drosophila pseudoobscura hybrids. Genetics. 21(2): 113.

587   Exposito-Alonso M., Vasseur F., Ding W., Wang G., Burbano H.A., & Weigel, D. 2018.
588   Genomic basis and evolutionary potential for extreme drought adaptation in
589   *Arabidopsis thaliana.* Nature ecology & evolution. 2(2):352.

591   Garroway C.J., Bowman J., Cascaden T.J., Holloway G.L., Mahan C.G., Malcolm J.R.,
592   Steele M.A., Turner G. & Wilson P.J. 2010. Climate change induced hybridization
593   in flying squirrels. Global Change Biology. 16(1):113-121.

595   Gerard P.R., Fernandez-Manjarres J.F., & Frascaria-Lacoste N.A. 2006. Temporal cline
596   in a hybrid zone population between *Fraxinus excelsior* L. and *Fraxinus angustifolia*
597   Vahl. Molecular Ecology. 15(12):3655-3667.

599   Gienapp P., Leimu R. & Merilä J. 2007. Responses to climate change in avian migration
600   time—microevolution versus phenotypic plasticity. Climate Research. 35(1-2):25-
601   35.

603   Gingerich P.D. 1993. Quantification and comparison of evolutionary rates. American
604   Journal of Science, 293(A):453-478

606   Gómez J.M., González-Megías A., Lorite J., Abdelaziz M. & Perfectti F. 2015. The silent
607   extinction: climate change and the potential hybridization-mediated extinction
608   of endemic high-mountain plants. Biodiversity and Conservation. 24(8):1843-
609   1857.

611   Gompert, Z., Parchman, T. L., & Buerkle, C. A. 2012. Genomics of isolation in hybrids.
612   Philosophical Transactions of the Royal Society of London B: Biological Sciences.
613   367(1587):439-450.

615   Haller B.C. & Messer P.W. 2018. SLiM 3: Forward genetic simulations beyond the
616   Wright–Fisher model, Molecular Biology and Evolution. msy228

618 Hendry A.P., Farrugia T.J. & Kinnison M.T. 2008. Human influences on rates of
619   phenotypic change in wild animal populations. Molecular Ecology. 17(1):20-29.
620

621 Hoffmann A.A. & Sgrò C.M. 2011 Climate change and evolutionary adaptation. Nature.
622   470(7335):479.
623

624 Jump A.S. & Penuelas J. 2005. Running to stand still: adaptation and the response of
625   plants to rapid climate change. Ecology Letters. 8(9):1010-1020.
626

627 Kingsolver, J.G., Hoekstra H.E., Hoekstra J.M, Berrigan D., Vignieri S.N., Hill C.E.,
628   Hoang A., Gibert P., & Beerli P. 2001. The strength of phenotypic selection in
629   natural populations. The American Naturalist. 3(157):245-261.
630

631 Lindtke, D. & Buerkle, C.A. 2015. The genetic architecture of hybrid incompatibilities
632   and their effect on barriers to introgression in secondary contact. Evolution.
633   69(8):1987-2004.
634

635 Lynch, M., & R. Lande. 1993. Evolution and extinction in re-sponse to environmental
636   change. Pp. 234-250 in P. M. Kareiva, J. G. Kingsolver, and R. B. Huey, eds. Biotic
637   interactions and global change. Sinauer, Sunderland, Mass.
638

639 Mallet J. 2005. Hybridization as an invasion of the genome. Trends in Ecology &
640   Evolution. 20(5):229-237.
641

642 Merilä, J., & Hoffmann, A.A. 2016. Evolutionary Impacts of Climate Change. In *Oxford*
643   *Research Encyclopedia of Environmental Science*. Oxford University Press.
644

645 Muller, H.J. 1942. Isolating mechanisms, evolution, and temperature. Biol. Symp. 6:71–
646   125.
647

648 Oliveira R., Godinho R., Randi E. & Alves P.C. 2008. Hybridization versus conservation:
649   are domestic cats threatening the genetic integrity of wildcats (*Felis silvestris*
650   *silvestris*) in Iberian Peninsula?. Philosophical Transactions of the Royal Society
651   of London B: Biological Sciences. 363(1505):2953-2961.
652

653 Pespeni M.H., Sanford E., Gaylord B., Hill T.M., Hosfelt J.D., Jaris H.K., LaVigne M.,
654   Lenz E.A., Russell A.D., Young M.K. & Palumbi S.R. 2013. Evolutionary change
655   during experimental ocean acidification. Proceedings of the National Academy of
656   Sciences. 110(17):6937-6942.

658 Pfennig KS. 2007. Facultative mate choice drives adaptive hybridization. Science.
659   318(5852):965-967.

661 R Core Team (2018). R: A language and environment for statistical computing. R
662   Foundation for Statistical Computing, Vienna, Austria. URL https://www.R-
663   project.org/.

665 Ravinet M., Faria R., Butlin R.K., Galindo J., Bierne N., Rafajlović M., Noor M.A.F.,
666   Mehlig B & Westram, A. M. 2017. Interpreting the genomic landscape of
667   speciation: a road map for finding barriers to gene flow. Journal of Evolutionary
668   Biology. 30(8):1450-1477.

670 Rhymer J.M. & Simberloff D. 1996. Extinction by hybridization and introgression.
671   Annual Review of Ecology and Systematics. 27(1):83-109.

673 Samuk K., Owens G.L., Delmore K.E., Miller S.E., Rennison D.J. & Schluter D. 2017.
674   Gene flow and selection interact to promote adaptive divergence in regions of
675   low recombination. Molecular Ecology. 26(17):4378-4390.

677 Savolainen O., Lascoux M., & Merilä J. 2013. Ecological genomics of local adaptation.
678   Nature Reviews Genetics. 14(11):807.

680 Seehausen, O. 2013. Conditions when hybridization might predispose populations for
681   adaptive radiation. Journal of Evolutionary Biology, 26(2), 279-281.

683 Schumer M., Xu C., Powell D.L., Durvasula A., Skov L., Holland C., Blazier J.C.,
684   Sankararaman S., Andolfatto P., Rosenthal G.G. & Przeworski, M. 2018. Natural
685   selection interacts with recombination to shape the evolution of hybrid genomes.
686   Science. 360(6389):656-660.

688 Taylor E.B., Boughman J.W., Groenenboom M., Sniatynski M., Schluter D. & Gow J.L.
689   2006. Speciation in reverse: morphological and genetic evidence of the collapse of
690   a three-spined stickleback (*Gasterosteus aculeatus*) species pair. Molecular
691   Ecology.15(2):343-355.
692

693 Thomas C.D., Cameron A., Green R.E., Bakkenes M., Beaumont L.J., Collingham Y.C.,
694   Erasmus B.F., De Siqueira M.F., Grainger A., Hannah L. & Hughes L. 2004.
695   Extinction risk from climate change. Nature. 427(6970):145.
696

697 Todesco M., Pascual M.A., Owens G.L., Ostevik K.L., Moyers B.T., Hübner S., Heredia
698   S.M., Hahn M.A., Caseys C., Bock D.G., Rieseberg L.H. 2016. Hybridization and
699   extinction. Evolutionary Applications. 9(7):892-908.
700

701 Vallender R., Robertson R.J., Friesen V.L. & Lovette I.J. 2007. Complex hybridization
702   dynamics between golden-winged and blue-winged warblers (*Vermivora*
703   *chrysoptera* and *Vermivora pinus*) revealed by AFLP, microsatellite, intron and
704   mtDNA markers. Molecular Ecology. 16(10):2017-2029.
705

706 Vonlanthen P., Bittner D., Hudson A.G., Young K.A., Müller R., Lundsgaard-Hansen B.,
707   Roy D., Di Piazza S., Largiadèr C.R. & Seehausen O. 2012. Eutrophication causes
708   speciation reversal in whitefish adaptive radiations. Nature. 482(7385):357.
709

710 Walther G.R., Post E., Convey P., Menzel A., Parmesan C., Beebee T.J., Fromentin J.M.,
711   Hoegh-Guldberg O. & Bairlein F. 2002 Ecological responses to recent climate
712   change. Nature. 416(6879):389.
713

714 Wickham H. 2016. ggplot2: elegant graphics for data analysis. Springer.
715

716 Yeaman S., Hodgins K.A., Lotterhos K.E., Suren H., Nadeau S., Degner J.C., Nurkowski
717   K.A., Smets P., Wang T., Gray L.K., Liepe K.J., Hamann A., Holliday J.A.,
718   Whitlock M.C., Rieseberg L.H. & Liepe K.J. 2016. Convergent local adaptation to
719   climate in distantly related conifers. Science. 353(6306):1431-1433.
720

721 Zamir D. 2001. Improving plant breeding with exotic genetic libraries. Nature reviews
722   genetics. 2(12):983–989.

723

724   Zimova M., Mills L.S. & Nowak J.J. 2016. High fitness costs of climate change-induced

725   camouflage mismatch. Ecology Letters. 19(3):299-307.

Supplemental Figures

727

728
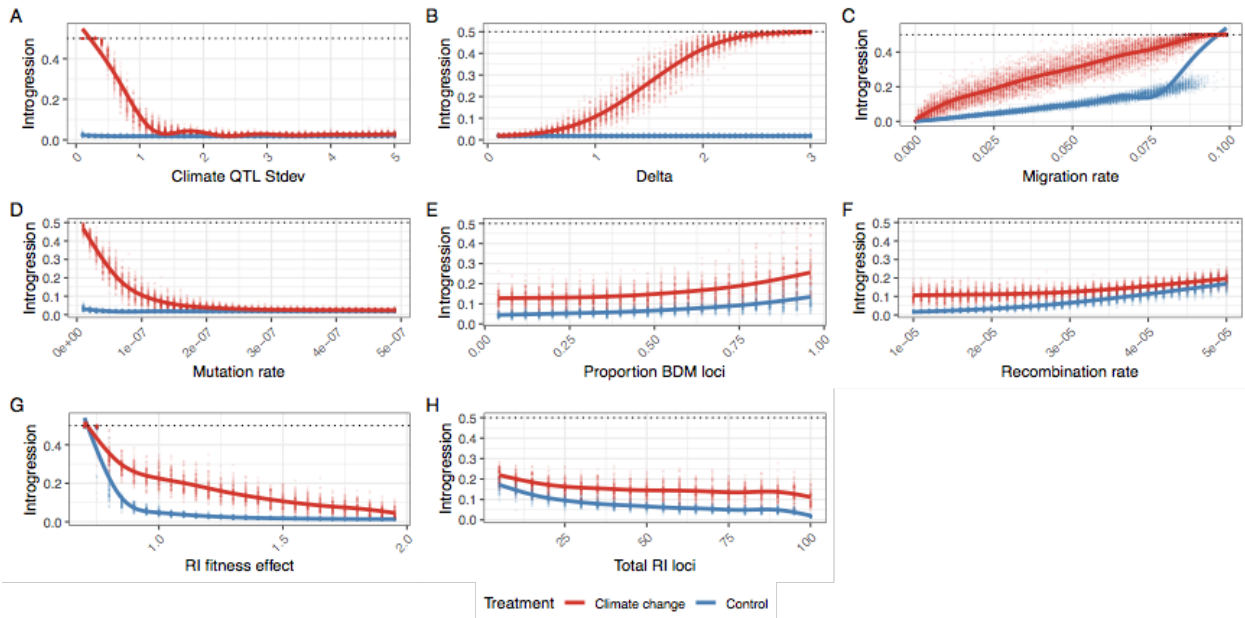
Figure S1 | The average amount of introgression at generation 10,100 for climate change (red) and control simulations (blue), while varying individual parameters. Complete homogenization of both populations occurs when average introgression = 0.5. Individual parameters were varied to show the effect of (A) climate QTL effect size standard deviation, (B) optimum shift per generation (delta), (C) migration rate, (D) climate QTL mutation rate, (E) proportion of RI loci that are BDM instead of extrinsic, (F) the recombination rate, (G) the fitness effect of each RI loci and (H) the number of RI loci.
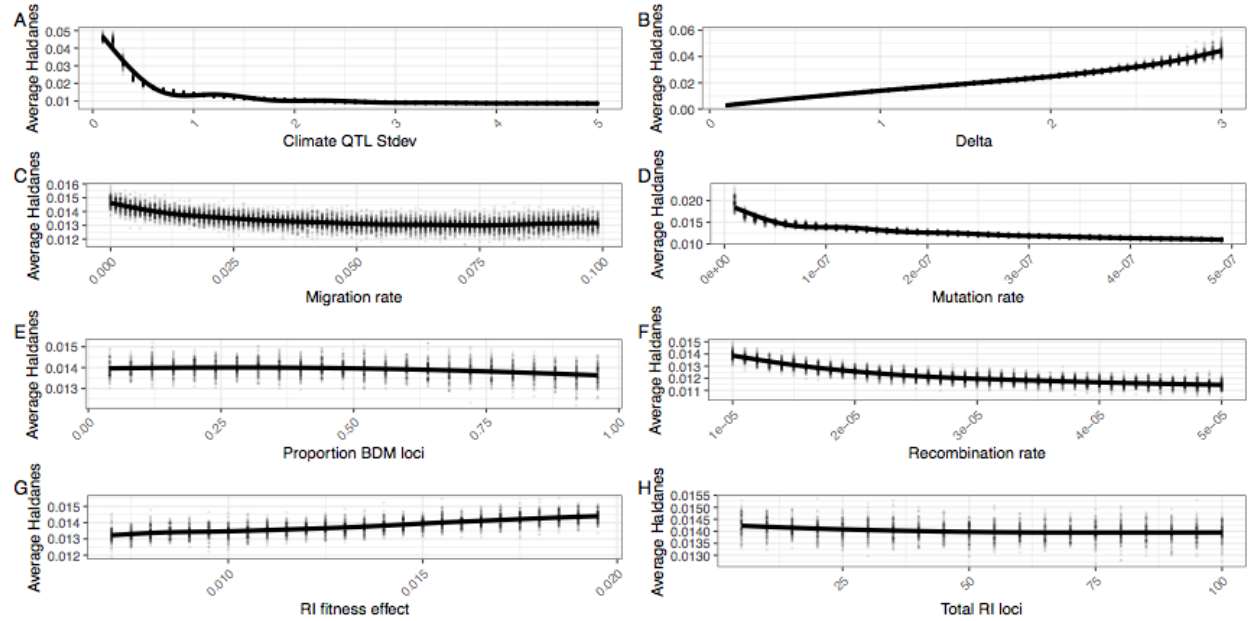
Figure S2 | The average Haldanes for the post-burn in period with climate change. Individual parameters were varied to show the effect of A) climate QTL effect size standard deviation, (B) optimum shift per generation (delta), (C) migration rate, (D) climate QTL mutation rate, (E) proportion of RI loci that are BDM instead of extrinsic, (F) the recombination rate, (G) the fitness effect of each RI loci and (H) the number of RI loci. Note that Haldanes are scaled by trait variation, so the same rate of absolute phenotypic change (i.e. Darwins) can have multiple different Haldanes if the phenotypic variability changes. In all panels except B, the rate of phenotypic change roughly matches the rate of environmental change, so the differences in Haldanes reflects differences in trait variance. Lower trait variance (e.g. through reduced mutation rate or lower QTL standard deviation) produces higher haldanes for the same absolute rate of phenotypic change.

Figure & Table Captions

Figure 1

(A) The genetic architecture of adaptation and speciation in the model. From left to right: Each individual has a single 100-1000 cM chromosome, over which reproductive isolation (RI) loci occur at regularly-spaced intervals. These loci are initialized with RI alleles (at 100% frequency) that confer local adaptation to one of two initial demes (depicted as green or purple/dotted alleles, corresponding to Deme 1 or Deme 2 environments). Both demes are of equal size (Ne = 1000). All non-RI loci (depicted as white/transparent loci, initially) have the potential to give rise to climate-adaptation alleles. The phenotypic effects of each these alleles are drawn from a normal distribution (shown as a gradient from blue to white to red). An individual's climate phenotype is the sum of the phenotypic effects of its climate QTLs (pure additivity). The fitness of each individual is a function of the number of foreign RI alleles and the phenotypic distance of that individual from the environmental optimum, with the climate fitness landscape modelled as a gaussian distribution (shown as a gradient from blue to red). (B) The course of the simulation. Migration rate and population size of the two demes is held constant. In each replicate simulation, the fitness optimum fluctuates regularly for a 10 000-generation burn-in period. The state of the initial population is then duplicated and subjected to 100 additional generations of (1) a climate change scenario in which the climatic optimum rapidly shifts in a single direction and (2) a control scenario in which the optimum continues its fluctuation course. (C) The conditions under which adaptive introgression overwhelms RI. On the left, if the two populations are able to individually track the climatic optimum, newly-arising climate alleles are only able to exert either weakly positive or (more commonly) negative effects on fitness due to overshooting the optimum. In contrast, on the right, if the populations cannot effectively track the optimum, there is scope for climatic alleles to have large positive fitness effects. If these fitness effects are sufficiently large, these alleles can overwhelm the negative fitness effects of linked RI alleles and introgress between demes, degrading overall reproductive isolation.

Figure 2

A single example simulation with Δ = 1.5, illustrating the climate driven adaptive introgression. Panels A-D present the test climate change scenario, while E-H are the control scenario. (A & E) The upper half is the average introgressed ancestry for each population (purple and green) and the average reproductive isolation between populations (black). The lower half is the ancestry for neutral loci during the post-burn in period at 20 generation intervals. The top and bottom parts of this portion represent population 1 and 2 respectively. (B & F) The allele frequency trajectory for introgressed climate QTL color coded by QTL strength. Color codes QTL effect; -ve phenotypic effect (blue), +ve effects (light red) or large +ve effect (>2, dark red). (C & G) The allele frequency trajectory for introgressed RI alleles (D & H) The distribution of selection coefficients on QTL loci per population per generation. Color groups represent QTL with -ve

791 phenotypic effect (blue), +ve effects (light red) or large +ve effect (>2, dark red). Plot is filtered to only

792 include loci with allele frequency < 0.9 and > 0.1.

793

794 **Figure 3**

795 The average reproductive isolation at generation 10,100 for climate change (red) and control simulations

796 (blue), while varying individual parameters. RI is defined as the home fitness advantage which is the fold

797 fitness advantage for the average sample in its home environment compared to the alternate environment

798 based on divergent selection and BDM loci. A value of 1 means equal fitness in both environments and

799 there is no RI. The black dot is the initial and maximum level of RI for each simulation. Individual

800 parameters were varied to show the effect of (A) climate QTL effect size standard deviation, (B) optimum

801 shift per generation (delta), (C) migration rate, (D) climate QTL mutation rate, (E) proportion of RI loci

802 that are BDM instead of extrinsic, (F) the recombination rate, (G) the fitness effect of each RI loci and (H)

803 the number of RI loci.

804

805 **Figure S1**

806 The average amount of introgression at generation 10,100 for climate change (red) and control simulations (blue),

807 while varying individual parameters. Complete homogenization of both populations occurs when average

808 introgression = 0.5. Individual parameters were varied to show the effect of (A) climate QTL effect size standard

809 deviation, (B) optimum shift per generation (delta), (C) migration rate, (D) climate QTL mutation rate, (E) proportion

810 of RI loci that are BDM instead of extrinsic, (F) the recombination rate, (G) the fitness effect of each RI loci and (H)

811 the number of RI loci.

812

813 **Figure S2**

814 The average Haldanes for the post-burn in period with climate change. Individual parameters were varied to show the

815 effect of A) climate QTL effect size standard deviation, (B) optimum shift per generation (delta), (C) migration rate,

816 (D) climate QTL mutation rate, (E) proportion of RI loci that are BDM instead of extrinsic, (F) the recombination rate,

817 (G) the fitness effect of each RI loci and (H) the number of RI loci. Note that Haldanes are scaled by trait variation, so

818 the same rate of absolute phenotypic change (i.e. Darwins) can have multiple different Haldanes if the phenotypic

819 variability changes. In all panels except B, the rate of phenotypic change roughly matches the rate of environmental

820 change, so the differences in Haldanes reflects differences in trait variance. Lower trait variance (e.g. through reduced

821 mutation rate or lower QTL standard deviation) produces higher haldanes for the same absolute rate of phenotypic

822 change.

823

824 **Table 1**

825 Parameters of the adaptive introgression simulations. For each set of simulations, each parameter was set

826 to the starting value which was varied from the minimum to maximum value by the specified increment.

35